

Role of orbital overlap in atomic manipulation

Sam Jarvis,¹ Adam Sweetman,¹ Joseph Bamidele,² Lev Kantorovich,² and Philip Moriarty¹

¹*The School of Physics and Astronomy, The University of Nottingham, Nottingham, NG7 2RD, United Kingdom*

²*Department of Physics, King's College London, The Strand, London, WC2R 2LS, United Kingdom*

(Received 7 November 2011; revised manuscript received 13 April 2012; published 7 June 2012)

We conduct *ab initio* simulations illustrating that the ability to achieve atomic manipulation using a dynamic force microscope depends on the precise orientation of the dangling bond(s) at the tip apex and their charge density with respect to those of surface atoms. Using the Si(100)- $c(4 \times 2)$ surface as a prototype, we demonstrate that it is possible to select tip apices capable of performing atomic manipulation tasks which are unachievable using another choice of apex. Specific tip apices can be identified via examination of $F(z)$ curves taken at different lateral positions.

DOI: [10.1103/PhysRevB.85.235305](https://doi.org/10.1103/PhysRevB.85.235305)

PACS number(s): 81.16.Ta, 68.37.Ps, 71.15.Mb, 81.05.Cy

I. INTRODUCTION

Atomic manipulation at the single-atom level using dynamic force microscopy (DFM) is becoming routine,¹⁻⁴ allowing extraordinary experiments to be realized on surfaces inaccessible by scanning tunneling microscopy, or in systems where DFM greatly assists single-atom precision. Nonetheless, due to the complex interaction between the scanning probe apex and surface atoms, atomic manipulation DFM remains fraught with difficulties and experimental unknowns. A major challenge in scanning probe microscopy (SPM), especially DFM, is to elucidate the exact nature and role of the tip-sample interaction, not only in the formation of image contrast, but, critically, during atomic manipulation.

Several explanations have been advanced to describe the origin of atomic resolution on reactive,⁵⁻⁷ metallic,^{8,9} and insulating materials.^{10,11} On reactive surfaces in particular, contrast is attributed to a weak chemical interaction between the surface and a dangling bond at the tip apex. On a given surface, a wide variety of stable image contrasts^{12,13} can be observed, and have been attributed to different tip apex structures possessing dangling bonds of varying spatial extent and electronic charge density. Just how tip structure then affects atomic manipulation has, however, thus far attracted little attention. Although Freitas and Merkle have carried out a comprehensive theoretical study of the tip types necessary to carry out fundamental mechanosynthetic¹⁴ reactions (i.e., atomic precision chemistry driven by mechanical force) on diamond surfaces,¹⁵ their simulated tip apices are rather complex and will necessitate challenging advances in controlling the chemistry of scanning probes. We focus here on simple prototypical systems and methods which are readily accessible by current experimental SPM methods.

Although it has been shown that a single tip can drive an exchange reaction between two atomic species at room temperature,⁴ such a process may not always be thermodynamically or kinetically viable. In the absence of an exchange reaction, the preference of an atom to bond to the probing tip or surface will be critical to extend the technique of DFM manipulation to arbitrary systems, and will be determined by the outermost tip orbital(s). The importance of the tip apex in high-resolution probe microscopy and atomic manipulation is well recognized, and has played a key role in a number of ground-breaking experiments^{4,16} which relied on a specific

probe termination. Accurate determination, functionalization, and control of the tip structure clearly represents the next hurdle to be surmounted in order to expand the possibilities of DFM and atomic manipulation.

In this paper we present calculations predicting that different tip types, modeled using small silicon tip clusters, undergo very different responses during atomic manipulation experiments due to the alignment, and the electronic charge density, of the atomic orbitals at the tip apex with respect to those of surface atoms. In our test system for vertical atomic manipulation, we attempt to deposit (extract) an atom onto (from) a surface. We observe that different classes of tip are able to perform only one of these manipulation steps, i.e., no single tip type considered here is capable of *both* atomic extraction *and* deposition. We illustrate how it may be possible to distinguish tip types via comparison of a line sequence of force-distance [$F(z)$] spectroscopy measurements.

The example model we choose is the manipulation of the Si(100) surface. At low temperatures the Si(100) surface reconstructs into a buckled dimer arrangement with a $c(4 \times 2)$ or $p(2 \times 2)$ periodicity,¹⁷⁻¹⁹ and we have previously shown that at 5 K the individual surface dimers can be manipulated from one buckled configuration to another.^{19,20} This system allows us to characterize the apex in an environment where atomic manipulation is entirely nondestructive, involving no removal of atoms or bond breaking, leaving the tip unaffected after manipulation. Si(100) also provides an ideal system for investigation of atomic manipulation in the form of the hydrogen-terminated Si(100):H surface.²¹

II. METHOD

Our investigation is performed with *ab initio* density functional theory simulations carried out using the SIESTA code²² using a double- ζ polarized basis set in the generalized gradient approximation (GGA) with a Perdew-Burke-Ernzerhof density functional, norm-conserving pseudopotentials, and a single $|\mathbf{k}| = 0$ point. The atomic structure was considered relaxed when forces on atoms fell below 0.01 eV/Å (for an extensive description please see Refs. 18–20). For all spectroscopy simulations the separation between the tip and surface, z , is defined as the vertical distance between the silicon apex of the tip structure and the surface upper dimer atom *prior* to relaxation to compare with experimental data. To represent

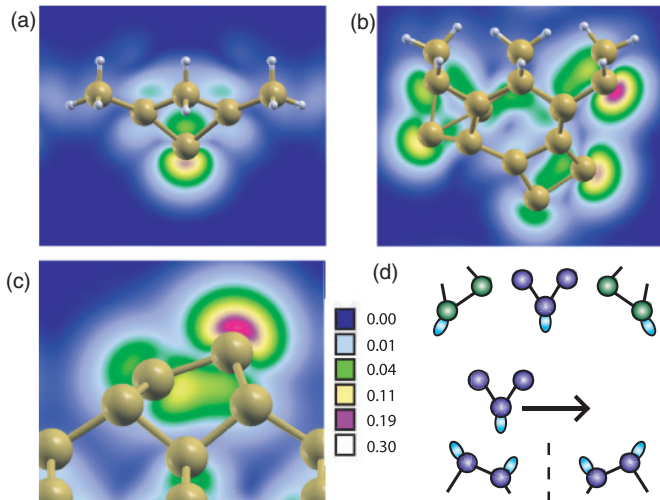


FIG. 1. (Color online) Ball-and-stick models of the H3 and dimer tips, and a Si(100) surface dimer, each overlaid onto their associated electronic charge density plot. (a) The H3 tip dangling bond is oriented parallel to the surface normal, whereas in (b) the dimer tip orbital is canted at an angle to the surface normal. The dimer tip can align or misalign with a surface Si(100) dimer [shown in (c)] depending on its orientation, and thus two extremes can be considered as distinct tips, where one apex is aligned with the surface dimer, while another is rotated by 180° around the surface normal relative to the other, yielding a misaligned tip. The scheme of simulations is shown in (d). Each of the three tips is laterally displaced between two dimers prior to simulating $F(z)$ spectra. Partial electron density plots are calculated from the states within the range 0–1 eV below the Fermi energy and plotted on a square root scale to aid clear visualization of the dangling bonds.

the Si(100) and Si(100):H surfaces a six-layer silicon slab model was used. A terminating hydrogen layer on the lower side of the slab was added and kept fixed along with the bottom two layers of silicon to simulate the missing bulk. For the H3 tip, four silicon atoms at the apex are free to move and for the dimerized tip fifteen. The tip clusters are moved relative to the surface in steps of 0.15 \AA ; the forces on all fixed tip atoms are then summed together at each step to produce $F(z)$.

Force-distance spectroscopy [$F(z)$] was simulated with the two tip structures depicted in Fig. 1: a Si(111)-type termination termed an ‘‘H3’’ tip, and a dimer-terminated cluster, both of which have been shown to provide accurate models of experimental AFM tip apices.^{6,7,12,23,24} Electron density plots (Fig. 1) show that the H3 apex represents an atomically rigid, symmetric tip termination with a single diffuse dangling bond pointing normal to the plane of the tip. The dimer tip is instead comprised of a less confined structure containing an angled and lower-charge-density apex dangling bond which can be aligned to a greater or lesser extent with the surface Si(100) dimer [Fig. 1(c)] depending on its orientation.²⁵

$F(z)$ spectroscopy has particular potential in obtaining information about the structure and symmetry of the tip apex. The effect of orbital alignment between the tip and surface is examined via three apex terminations: the H3 tip pointing normal to the surface plane, and two rotations of the dimer tip oriented 180° relative to each other. These terminations are depicted in Fig. 1(d). Critically, both tip and surface

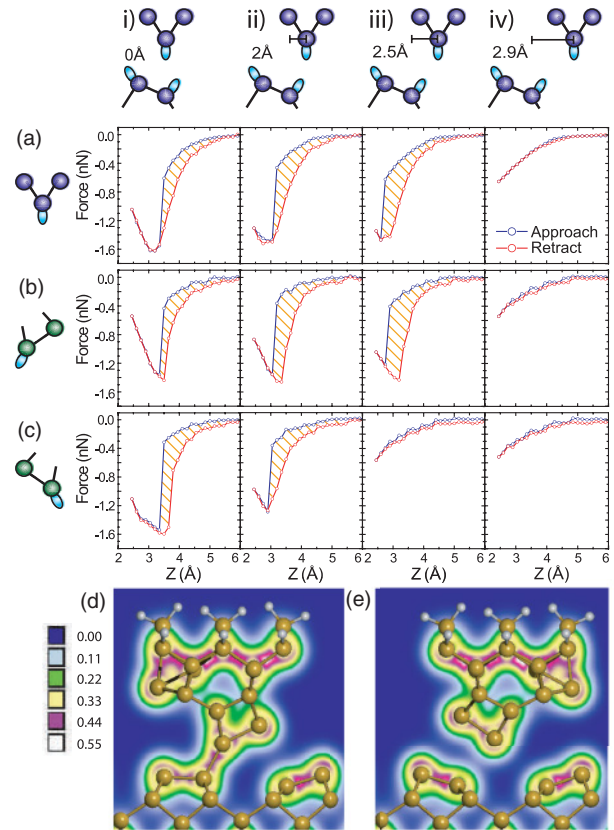


FIG. 2. (Color online) Effect of laterally positioning tips with directionally dependent dangling bond terminations. The (a) H3 and two rotated dimer tips [(b) aligned and (c) misaligned] are positioned directly above a lower dimer atom, and then displaced in steps indicated by schematics (i)–(iv). Clear variations in hysteresis are seen for the dimer tip when aligned (misaligned) with a surface dimer. Electron density plots corresponding to the force curves in (b,ii) and (c,iii), with, (d) an aligned, and (e) a misaligned tip, demonstrate the absence of bonding for one rotation of the dimer tip relative to the other.

dangling bonds protrude at an angle relative to the surface normal. This inherent symmetry between tip and surface leads to a very strong alignment or misalignment of the orbitals between the dimerized tip apex and surface dimer, depending on tip orientation, allowing simple examination of the role this plays in manipulation. To accomplish this, the tip is positioned such that its outermost apex atom is placed directly over the lower atom of the surface dimer, and then laterally offset in the direction between two adjacent Si(100) rows in steps of 0.5 \AA until the center point between rows is reached. Simulated spectroscopy was then carried out at each position, producing the calculated $F(z)$ curves in Fig. 2.²⁶

III. RESULTS

Plotted in Fig. 2(a) is a row of $F(z)$ curves each taken with the H3 tip apex laterally offset from the lower dimer atom as shown in the diagrams (i)–(iv). A steep vertical drop in the approach curves, in addition to the observation of force hysteresis, are clear signs of a successful surface dimer flip induced by the AFM tip. Due to the symmetry of the H3

tip, rotation about the normal axis produces no change in the $F(z)$ curves. Rotation of the dimer apex [Figs. 2(b) and 2(c)], however, results in distinct variation in the observed hysteresis. In the case (b) where the dimer tip is aligned with the surface dimer, hysteresis in the $F(z)$ curves is seen to increase in magnitude as the tip is offset from the lower dimer atom until the point where the tip no longer comes close enough to the surface dimer to form a strong interaction (i.e., ~ 2.9 Angstroms the center point between rows). The misaligned tip (c) demonstrates a continuous reduction in hysteresis, however, more rapidly reaching a point where surface dimer manipulation no longer occurs. On buckled surfaces such as Ge(100) and Si(100) this protocol could be experimentally implemented by taking a line of $\Delta f(z)$ spectroscopy measurements between lower dimer atoms on adjacent $c(4 \times 2)$ rows. Once the manipulation has taken place, the dimer could then be flipped back into its original configuration¹⁹ and the line spectra continued. The lower dimer atoms from adjacent rows can be used as convenient markers to check the symmetry of the $\Delta f(z)$ curves, or more usefully, of $F(z)$ curves extracted from the frequency shift measurement. *If distinct markers are used in this way, experimental knowledge about the exact tip apex atomic position is not required as this will not affect trends in the observed hysteresis.* The same is true regarding knowledge of the orientation of a dimer type tip. Provided that the tip is not aligned 90° relative to the surface dimers in adjacent rows (removing its asymmetry), some trend in the $F(z)$ curves should always be observed, identifying the structure as different from the symmetric H3 tip. Information about the symmetry of the AFM tip apex can therefore be obtained, and hence yield a general classification of the tip structure present. If the desired tip type has not been identified, then the typical⁴ trial-and-error approach of tip modification must be pursued. At each stage characterization of the tip can be made until the desired termination is obtained. It is also possible that automated probe optimization methods²⁷ could help facilitate this process.

In Figs. 2(d) and 2(e) total electron density plots are shown for two primary orientations (aligned and misaligned) of the dimer apex when laterally offset by 2.5 \AA and positioned in z at the closest point of approach in the $F(z)$ curves. Despite positioning the apex atom in exactly the same location prior to spectroscopy, we observe that the aligned tip interacts strongly enough to manipulate the surface dimer whereas a misaligned tip does not. This variation at 2.5 \AA lateral offset is likely a direct consequence of the unfavorable orientation of the tip, effectively increasing the distance between dangling bonds of the apex and lower dimer atoms such that the interaction is too weak to instigate manipulation. The differences in hysteresis can also be attributed to changes in how favorably the tip is aligned with the surface dimer. For the case of the tip orbital aligned parallel to that of the surface (b), the tip-surface bond forms in a location which is already favorable to the creation of a strong bond. In the case of the misaligned tip (c) the opposite is true, and the bond made will be considerably weaker. This procedure could in principle be extended to any situation where a dangling bond protrudes at an angle to the surface plane normal, such as natural surface reconstructions (e.g., buckled surfaces), surface defects, vacancies, or deposited atoms/molecules. Even in the absence of hysteresis from

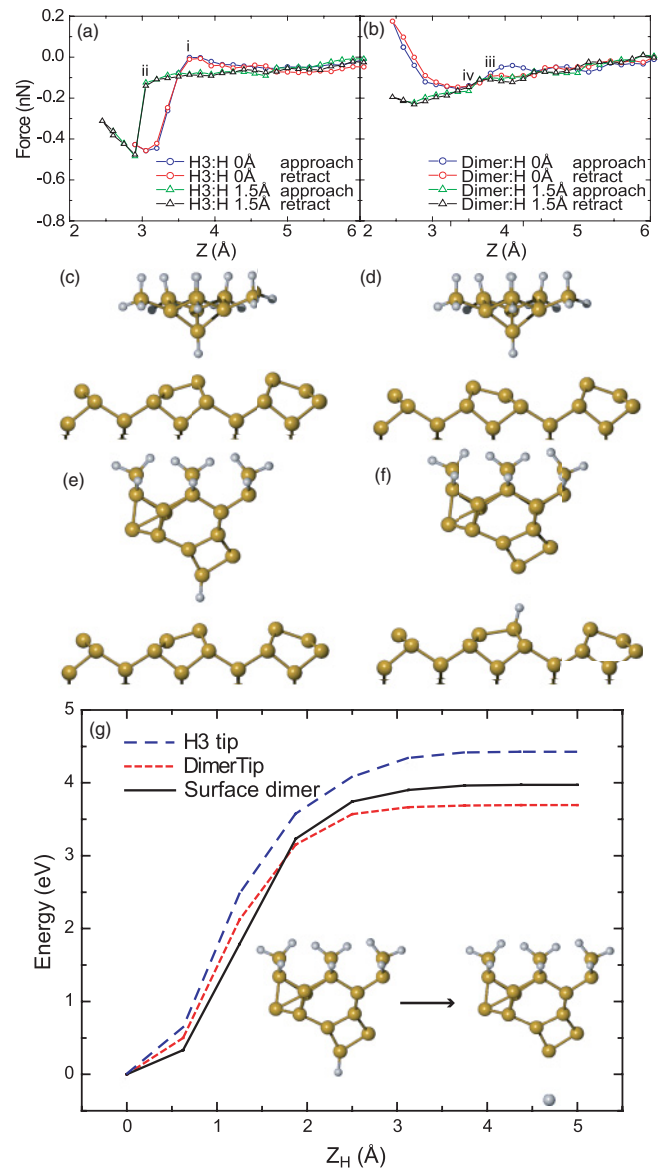


FIG. 3. (Color online) Atomic deposition (extraction) dependence on tip type. The H3 and dimerized tip structures have their apex dangling bond terminated with hydrogen to simulate the simplest possible atom deposition (extraction) experiment. Calculated force curves are shown for an (a) H3 and (b) dimer tip at two different lateral positions corresponding to 0 \AA and 1.5 \AA offset. Snap shots at 0 \AA offset show H3 (c),(d) [dimer (e),(f)] tip at point (i) [(iii)] on the force curve during approach and retraction, illustrating that the tip has retained (deposited) the hydrogen. In (g) we show the minimum energy pathway for removing a hydrogen atom from the surface upper dimer atom and from each tip type to a position of $Z_H = 5 \text{ \AA}$ away as shown in the inset. The Z_H scale represents the displacement of the hydrogen from its equilibrium bonding position.

atomic manipulation, purely tip-dependent hysteresis²⁸ could be studied in its place.

To examine a wider range of atomic manipulation events we also considered the extraction/deposition of a single H atom, enabling an analysis of atomic manipulation involving a competition between a reactive tip and surface. We performed

simulated force spectroscopy with the hydrogen-passivated H3 and dimer tips positioned (centered and laterally offset) above an upper Si(100) surface dimer atom. Figure 3 displays the calculated $F(z)$ curves for the (a) H3 and (b) dimer tips along with before (c),(e) and after (d),(f) ball-and-stick snapshots, at positions (a,i) and (b,iii) on approach and retraction. The simulations reveal that the two tip types generate different outcomes of manipulation: the H3 apex retains the bonded hydrogen atom, despite being driven far enough into the surface to *push* a dimer into its alternative configuration, whereas the dimer apex relinquishes its hydrogen, passivating the surface. Interestingly, in this case, the orientation of the dimer tip has no effect on the success of manipulation. Therefore, if the suggested tip characterization method was implemented, the particular orientation of the tip with respect to the surface does not need to be known. The ability to *push* a Si(100) dimer into its alternative configuration appears to be made possible only with a strongly bound, passivated tip such as the H-passivated H3 apex. Any tip type with a reactive apex would remain strongly bound to the surface dimer after approach, “pulling” it back up into its original position upon retraction of the tip.

Although the local electronic surface structure will differ, parallels can be drawn between the hydrogen-terminated H3 tip and a fully hydrogen-passivated Si(100) surface. If the strength of interaction between the H3 tip and hydrogen is strong enough to prevent passivation of a clean Si(100) surface, it may be reasonable to expect that a clean H3 tip could then be strong enough to extract a single hydrogen from a fully passivated Si(100):H surface. Such a manipulation would be unachievable using a dimer-class tip under the same conditions. This highlights the possible difficulty in performing vertical manipulation with DFM in some systems. In the absence of probabilistic processes allowing both atom deposition (extraction) with the same tip, experiments in systems with chemically dissimilar species may not be possible with standard methods alone.

A nudged elastic band (NEB) method was implemented to calculate the minimum-energy pathway for desorption of the hydrogen atom. The pathway is simple and intuitive, such that the barrier calculated by the NEB calculation is equivalent to the adsorption energy of the H atom. As shown in Fig. 3(g), hydrogen is more strongly bound to the H3 tip than to the surface, and more weakly bound to the dimerized tip. This result supports our observation that once the simulated tip structure is positioned at small tip-sample separations upon retraction, the atom undergoing manipulation remains bonded to the structure with the highest binding energy. We therefore conclude that the type of atomic manipulation that can be performed is determined by the reactivity of the tip apex with the target atom, relative to the surface.

The lateral positioning of the tips in this case had no significant influence on the success of manipulation. The $F(z)$ curves [shown in Figs. 3(a) and 3(b) for 0 Å and 1.5 Å lateral offset] demonstrated broadly the same behavior, and were simply offset in z by an amount corresponding to the larger core-core distance between tip and surface atom (for the dimer tip, a large positive increase in force is driven by the interaction becoming strongly repulsive at small tip-sample separations). For the Si(100) system we have considered, the differences in binding energy are too large to be affected by lateral positioning of the simulated AFM tip. It may be possible, however, that in other systems the energy balance may be more subtle, allowing back and forth manipulation to be realized using a lateral offsetting technique.

The $F(z)$ curves corresponding to the H3 tip contain an expected jump in measured force when the hydrogen atom is forced to bond to both the tip and surface [(i) and (ii) in Fig. 3(a)]. This is coupled with a lack of hysteresis confirming that no permanent change to the tip has taken place. Conversely, in the case of the dimer tip there is no such sudden change in force when the hydrogen atom is transferred [(iii) and (iv) in Fig. 3(b)] and, remarkably, no hysteresis. This unexpected behavior appears to originate from a lack of major structural rearrangement of the tip and surface following transfer of the atom. As shown in Figs. 3(e) and 3(f) very little change in the geometry of the tip and surface is observed; therefore it is perhaps unsurprising that the calculated forces are similar upon retraction. Additionally, surface modifications also appear to have minimal effect on the $F(z)$ curves.

IV. CONCLUSION

The results presented here demonstrate that it is possible to obtain distinct classes of tip apex which enable specific atomic manipulation processes, while precluding others. Simple protocols based around $F(z)$ spectroscopy enable a characterization and, in principle, selection of tip “tools” configured for particular classes of manipulation event.

ACKNOWLEDGMENTS

P.J.M. thanks the Engineering and Physical Sciences Research Council (EPSRC) for the award of a fellowship (No. EP/G007837/1). S.J. and J.B. also thank EPSRC for Ph.D. studentships. We also acknowledge funding from the European Commission’s ICT-FET programme via the “Atomic Scale and Single Molecule Logic gate Technologies (AtMol)” project, Contract No. 270028, and from the Leverhulme Trust through Grant No. F00-114/BI and the support of the University of Nottingham High Performance Computing Facility.

¹M. Ternes, C. P. Lutz, C. F. Hirjibehedin, F. J. Giessibl, and A. J. Heinrich, *Science* **319**, 1066 (2008).

²N. Oyabu, O. Custance, I. Yi, Y. Sugawara, and S. Morita, *Phys. Rev. Lett.* **90**, 176102 (2003).

³Y. Sugimoto, P. Jelínek, P. Pou, M. Abe, S. Morita, R. Pérez, and O. Custance, *Phys. Rev. Lett.* **98**, 106104 (2007).

⁴Y. Sugimoto, P. Pou, O. Custance, P. Jelínek, M. Abe, R. Pérez, and S. Morita, *Science* **322**, 413 (2008).

- ⁵F. J. Giessibl, *Science* **267**, 68 (1995).
- ⁶R. Pérez, M. C. Payne, I. Štich, and K. Terakura, *Phys. Rev. Lett.* **78**, 678 (1997).
- ⁷R. Pérez, I. Štich, M. C. Payne, and K. Terakura, *Phys. Rev. B* **58**, 10835 (1998).
- ⁸P. Dieška, I. Štich, and R. Pérez, *Phys. Rev. Lett.* **91**, 216401 (2003).
- ⁹P. Dieška, I. Štich, and R. Pérez, *Nanotechnology* **15**, S55 (2004).
- ¹⁰A. S. Foster, C. Barth, A. L. Shluger, and M. Reichling, *Phys. Rev. Lett.* **86**, 2373 (2001).
- ¹¹A. S. Foster, A. Y. Gal, J. D. Gale, Y. J. Lee, R. M. Nieminen, and A. L. Shluger, *Phys. Rev. Lett.* **92**, 036101 (2004).
- ¹²N. Oyabu, P. Pou, Y. Sugimoto, P. Jelínek, M. Abe, S. Morita, R. Pérez, and O. Custance, *Phys. Rev. Lett.* **96**, 106101 (2006).
- ¹³A. Sweetman, S. Jarvis, R. Danza, and P. Moriarty, *Beilstein J. Nanotechnol.* **3**, 25 (2012).
- ¹⁴K. E. Drexler, *Nanosystems: Molecular Machinery, Manufacturing, and Computation* (John Wiley and Sons, New York, 1992).
- ¹⁵R. A. Freitas and R. C. Merkle, *J. Comput. Theor. Nanosci.* **5**, 760 (2008).
- ¹⁶L. Gross, F. Mohn, N. Moll, P. Liljeroth, and G. Meyer, *Science* **325**, 1110 (2009).
- ¹⁷R. A. Wolkow, *Phys. Rev. Lett.* **68**, 2636 (1992).
- ¹⁸Y. J. Li, H. Nomura, N. Ozaki, Y. Naitoh, M. Kageshima, Y. Sugawara, C. Hobbs, and L. Kantorovich, *Phys. Rev. Lett.* **96**, 106104 (2006).
- ¹⁹A. Sweetman, S. Jarvis, R. Danza, J. Bamidele, S. Gangopadhyay, G. A. Shaw, L. Kantorovich, and P. Moriarty, *Phys. Rev. Lett.* **106**, 136101 (2011).
- ²⁰A. Sweetman, S. Jarvis, R. Danza, J. Bamidele, L. Kantorovich, and P. Moriarty, *Phys. Rev. B* **84**, 085426 (2011).
- ²¹J. Boland, *Adv. Phys.* **42**, 129171 (1993).
- ²²J. M. Soler, E. Artacho, J. D. Gale, A. García, J. Junquera, P. Ordejón, and D. Sánchez-Portal, *J. Phys.: Condens. Matter* **14**, 2745 (2002).
- ²³P. Pou, S. A. Ghasemi, P. Jelínek, T. Lenosky, S. Goedecker, and R. Pérez, *Nanotechnology* **20**, 264015 (2009).
- ²⁴R. Bechstein, C. González, J. Schütte, P. Jelínek, R. Pérez, and A. Kühnle, *Nanotechnology* **20**, 505703 (2009).
- ²⁵We note that although the charge distribution at the apex dimer atoms is qualitatively similar to that in previous work (Ref. 23), our relaxed geometry suggests that charge is transferred in the opposite direction—away from the apex. We attribute this to the use of the GGA, as opposed to the local density approximation, and a larger basis set producing a subtly wider tip apex.
- ²⁶Note that the tip-sample separation used as the abscissa in Figs. 2 and 3 does not represent a “true” reaction coordinate. The variation in force is plotted this way to aid direct comparison with experiment.
- ²⁷R. A. J. Woolley, J. Stirling, A. Radocea, N. Krasnogor, and P. Moriarty, *Appl. Phys. Lett.* **98**, 253104 (2011).
- ²⁸S. A. Ghasemi, S. Goedecker, A. Baratoff, T. Lenosky, E. Meyer, and H. J. Hug, *Phys. Rev. Lett.* **100**, 236106 (2008).